移动扫码阅读

韩丹丹,胡胜勇,张 慕,等.采空区垮落岩体空隙率分布规律及其形成机理研究[J].煤炭科学技术,2020,48(11):113-120. doi:10.13199/j.cnki.cst.2020.11.014

HAN Dandan,HU Shengyong,ZHANG Ao,*et al*.Study on voidage distribution regulation and formation mechanism of crushed rock mass in gob[J]. Coal Science and Technology, 2020, 48(11): 113-120. doi: 10.13199/j.cnki.cst.2020.11.014

采空区垮落岩体空隙率分布规律及其形成机理研究

韩丹丹,胡胜勇,张 慕,郝国才,胡岚清

(太原理工大学 安全与应急管理工程学院,山西 太原 030024)

摘 要:基于岩块间应力的传递和演化会改变采空区垮落岩体的密实程度,进而影响垮落岩体空隙的分布,最终影响采空区瓦斯的流动特性,为了解采空区瓦斯运移通道,获得控制瓦斯流动的理论依据,基于离散单元法,采用 Hertz-Mindlin 接触模型,通过自编程序,分别模拟了直径为 0.6、0.8、1.0 m 的岩块组成的垮落岩体在轴向应变为 0、0.05、0.10、0.15、0.20 和 0.25 下的压实过程,研究了采空区垮落岩体内应力是如何通过改变岩块间的接触网络来影响垮落岩体空隙率的分布。研究结果表明:垮落岩体内应力通过岩块间的接触网络进行传递,随轴向应变增大,垮落岩体内应力逐渐增大,传递应力的接触网络也越密集;压缩过程中,外部载荷无法从垮落岩体顶部的受力端均匀地传递到下部,使垮落岩体上部岩块受力大于下部,且随轴向应变增大,岩块间接触力较大的区域自垮落岩体上部向下不断扩展;由于垮落岩体下部岩块受外力扰动小,使垮落岩体下部岩块间的接触网络较疏松,配位数较小。垮落岩体自下向上空隙率先急剧降低,随后缓慢下降。其中自然堆积状况下,垮落岩体因自重所产生的应力较小,不同层位岩块的配位数相差较小,使垮落岩体底部空隙率仅为上部空隙率的 1.1 倍。而在压实状况下,垮落岩体不同层位岩块受力相差较大,垮落岩体底部岩块的配位数远小于垮落岩体上部,导致垮落岩体底部空隙率是上部空隙率的 1.4 倍。

关键词:采空区;垮落岩体;外部载荷;配位数;空隙率

中图分类号:TD313.7;TD712.52 **文献标志码**:A **文章编号**:0253-2336(2020)11-0113-08

Study on voidage distribution regulation and formation mechanism of crushed rock mass in gob

HAN Dandan,HU Shengyong,ZHANG Ao,HAO Guocai,HU Lanqing

(*College of Safety and Emergency Management Engineering,Taiyuan University of Technology,Taiyuan* 030024,*China*)

Abstract:The transfer and evolution of stress between rock blocks will change the compactness of crushed rock mass in the gob,and then affect the void distributions of crushed rock mass,and finally change the flow of gas in the gob.In this paper,a discrete element method was used,along with the Hertz-Mindl in contact model and self-programming.The compaction processes of crushed rock mass composed of rock blocks with diameters of 0.6 0.8 and 1.0 m were simulated,with axial strains set at 0、0.05、0.10、0.15、0.20,and 0.25,respectively.The goal of this study was to study how the internal stress of crushed rock mass in the gob affected the void distribution of crushed rock mass by changing the contact network between the rock blocks.The results showed that the stress in crushed rock mass was transmitted through the contact network between the rock blocks,and as the axial strains increased,the stress in the crushed rock mass increased gradually,and the contact network that transmitted the stress became denser.During the compression process,the external load could not be uniformly transmitted from the top of the crushed rock mass to the lower part,so that the stress in upper part of the crashed rock mass was significantly higher than the lower part.As the axial strains increased,the range with large contact force between the rock blocks gradually expanded from the upper part of the rock mass to the lower part.Because the rock blocks in the lower part of the crushed rock mass wasless interfered by the external force,the contact network between the rock blocks in the lower part of the crushed rock mass was looser,and the coordina-

收稿日期:2019-12-12;**责任编辑**:曾康生

基金项目:国家自然科学基金资助项目(51504160)

作者简介:韩丹丹(1994—),女,河北邢台人,硕士研究生。E-mail:1787451535@qq.com

通讯作者:胡胜勇(1984—),男,湖北随州人,副教授,博士生导师。E-mail:hsyztx@163.com

tion number of the rock blocks in the lower part of the crushed rock mass was small. The void rate of the crushed rock mass decreased sharply from bottom to top, and then slowly decreased. Under the natural accumulation condition, the stress generated by the self-weight of crushed rock mass was small, and the coordination number of rock blocks in different layers was relatively small, so that the voidage at the bottom of the crushed rock mass was only 1.1 times that in the upper of crushed rock mass. However, under compaction conditions, the stress in different layers of the crushed rock mass had a large difference, and the coordination number of the rock blocks at the bottom of crushed rock mass was much smaller than that of the upper part, so that the voidage at the bottom of the crushed rock mass was 1.4 times that in the upper of crushed rock mass.

Key words: gob; crushed rock mass; external load; coordination number; voidages

0 引　　言

受遗煤、煤壁与邻近煤层的影响,采空区积存大量瓦斯[1-4],采空区岩块群形成的多孔介质为瓦斯涌入工作面提供了运移通道[5-7],采空区瓦斯的大量涌出严重威胁工作面的安全。采空区不同位置的垮落岩体受力存在明显区别[8],远离工作面方向,采空区垮落岩体的上覆载荷逐渐增大,垮落岩体更加密实,垮落岩体内的空隙逐渐变小,导致瓦斯的运移通道发生改变。采空区上覆载荷通过改变垮落岩体的密实程度,影响岩块间空隙分布特征,最终改变采空区瓦斯的流动特性[9-10]。因此研究上部载荷对采空区垮落岩块间空隙分布特征的影响,对了解采空区瓦斯运移通道,控制瓦斯流动提供了理论依据。

国内外学者在采空区垮落岩体应力对空隙率的影响方面开展了大量研究。陈占清等[11]利用破碎岩石渗透特性试验系统,研究了蠕变过程中孔隙度的变化率;樊秀娟等[12]利用岩石承压变形仪,研究了岩体变形与岩块粒径、轴向应力的关系;张季如等[13]通过侧限压缩试验,研究了孔隙比随应力的变化规律;孟召平等[14]研究了不同含水状态下砂岩应力与应变之间的关系;梁运涛等[15]研究了采空区倾斜方向上空隙率的二维分布规律;徐俊明等[16]采用自行设计的压实装置,分析了压实过程中矸石与粉煤灰的变形特征;苏承东等[17]通过碎石压实试验,研究了岩块粒径与碎胀系数关系;王少锋等[18]通过构建采场覆岩下沉连续曲面数学模型,研究了采空区空隙率的三维分布规律;冯梅梅等[19]利用自制的力学压实装置,研究了应力与破碎岩石孔隙率之间的关系;WANG 等[20]通过理论计算和数值模拟,推导出采空区空隙率的分布特征;孟召平等[3]根据破碎岩体孔隙率和碎胀系数关系,建立了采空区垮落带内岩体孔隙的体积模型;孙利辉等[21]利用破碎岩石压实装置,研究了岩块块度与碎胀系数的关系;褚廷湘等[22]研究了破碎煤块碎胀系数与轴向应力之间的关系;张俊文等[23]利用自制的岩石承压变形装置,研究了破碎岩块空隙率与应力之间关系。上述研究成果仅从宏观上研究外部载荷对垮落岩体空隙率的影响,鲜有研究在外部载荷作用下,细观尺度下垮落岩体内应力如何改变岩块间的接触网络,来影响垮落岩体内不同层位空隙率的分布。

基于离散单元法,采用 Hertz-Mindlin 接触模型,运用自编程序,模拟垮落岩体在轴向应变为 0、0.05、0.10、0.15、0.20 和 0.25 下的压实过程,分析了不同压实程度下,垮落岩体内应力自上向下传递过程中配位数的分布及演化特征,研究了岩体内不同层位空隙的分布。

1 数值模拟方法

1.1 数学模型

采用采用 Hertz-Mindlin 接触模型,模拟岩块间的受力及岩块的运移。

岩块线加速度 $\dot{v}_i(t)$ 为

$$\dot{v}_i(t)=\frac{1}{\Delta t}[v_i(t+\Delta t/2)-v_i(t-\Delta t/2)] \tag{1}$$

岩块角加速度 $\dot{\omega}_i(t)$ 为

$$\dot{\omega}_i(t)=\frac{1}{\Delta t}[\omega_i(t+\Delta t/2)-\omega_i(t-\Delta t/2)] \tag{2}$$

岩块线速度 $v_i(t)$ 为

$$v_i(t)=v_i(t-\Delta t)+[F_i(t)/m+g_i]\Delta t \tag{3}$$

岩块角速度 $\omega_i(t)$ 为

$$\omega_i(t)=\omega_i(t-\Delta t)+(M_i(t)\Delta t/I) \tag{4}$$

岩块的合力矩 M_i 为

$$M_i=I\dot{\omega}_i=\frac{2}{5}mR^2\dot{\omega}_i \tag{5}$$

岩块接触力 F_i 为

$$F_i=F_i^{(n)}+F_i^{(p)} \tag{6}$$

颗粒间法向接触力 $F_{ni}^{(n)}$ 为

$$F_i^{(n)}=-k\delta_i^{(n)}-\eta^{(n)}v_i^{(n)} \tag{7}$$

颗粒间切向接触力 $F_i^{(p)}$ 为

$$F_i^{(p)}=-k^{(p)}\delta_i^{(p)}-\eta^{(p)}v_i^{(p)} \tag{8}$$

式中:$\dot{v}_i$ (+)为岩块 i 的线加速度,m/s^2;g 为重力加速度,m/s^2;$\dot{\omega}_i$ 为岩块 i 的角加速度,rad/s^2;v_i 为岩

块 i 的线速度,m/s;ω_i 为岩块 i 的角速度,rad/s;m 为岩块质量,kg;t 为时间变量,s;Δt 为时间变化量,s;I 为岩块转动惯量,kg·m^2;M 为岩块的力矩,N·m;$\boldsymbol{n}$ 为单位法向量;$\boldsymbol{p}$ 为单位切向量;δ 为岩块变形量,m;η 为阻尼系数,N·s/m;k 为弹性系数,N/m;F 为岩块间接触力,N;R 为岩块的半径,m。

1.2　物理模型

以山西霍州煤电李雅庄矿 2-607 工作面采空区为原型,其中 2-607 工作面采空区垮落带的高度约为 10 m。由于 2-607 工作面采空区的长度与宽度较大,将采空区抽象为 10 m × 10 m × 10 m 的垮落岩体单元,模拟采空区上覆岩层作用下,采空区不同位置垮落岩体的受力状态,如图 1 所示。

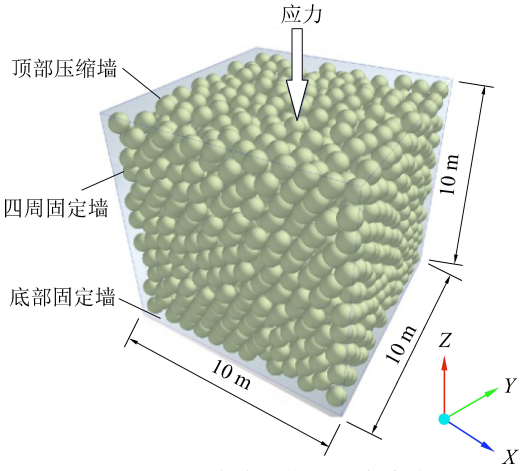

图 1　三维岩块群物理压缩模型

Fig.1　Three-dimensional rock blocks group physical compression model

为约束岩块的运动,模型四周与底部为固定边界墙。岩块自正方体模型顶部向下掉落,当正方体模型被充满后,在外部载荷作用下模型顶部的边界墙自上向下压缩垮落岩体,直到垮落岩体轴向应变 ε 分别达到 0、0.05、0.10、0.15、0.20 和 0.25 时停止。根据 2-607 工作面采空区岩块的实际力学特征,选定本次数值模拟岩块的参数如下:

泊松比	0.35
岩块密度/(kg·m^{-3})	2 200
剪切模量/(N·m^{-2})	1.85×10^9
阻尼系数/(N·s·m^{-1})	0.3
静摩擦因数	0.1
动摩擦因数	0.05

2　数值结果与分析

2.1　岩块受力

岩块间接触力演化云图如 2 所示。由图 2 可知:随垮落岩体轴向应变的增大,岩块间的接触力不断增大。当垮落岩体的轴向应变为 $\varepsilon=0$ 时,垮落岩体以蓝色区域为主,岩块间的接触力较小。当垮落岩体轴向应变为 $\varepsilon=0.05$ 时,由于外部载荷无法从垮落岩体顶部的受力端均匀地传递到岩体下部,使仅在垮落岩体上部出现小范围绿色区域,而垮落岩体的中下部仍以蓝色区域为主,表明垮落岩体上部岩块间的接触力要大于中下部。随轴向应变的增大,垮落岩体上部绿色区域不断向下部延展,岩块间接触力较大的区域自垮落岩体上部向下不断扩展。

将垮落岩体自下而上每 1 m 划分为一个单元,由于垮落岩体压缩 25%后的高度为 7.5 m,因此在此仅分析 7 m 高的垮落岩体内岩块间平均接触力,如图 3 所示。由图 3 可知:由于外部载荷难以自岩体顶部的受力端均匀的传递到岩体底部,使垮落岩体上部岩块受外部载荷扰动较大,导致垮落岩体内岩块间接触力自下而上整体呈上升趋势。岩体轴向应变从 0 增加到 0.25 过程中,由于岩块间的挤压和摩擦作用增强,导致岩块间的接触力也不断增大。

2.2　岩块细观特征配位数的分布

垮落岩体内某一岩块可能与周围一个或多个岩块相互接触,配位数为目标岩块与周围岩块接触的个数,平均配位数为垮落岩体内岩块的总配位数与岩块数量的比值,配位数则在细观尺度下表征垮落岩体的密实程度[24-25]。外部载荷作用下,垮落岩体内应力通过岩块间的接触网络进行传递,岩块的配位数体现了垮落岩体细观结构的密实程度,岩块配位数越大,垮落岩体内传递应力的接触网络就越密集。垮落岩体内岩块配位数的演化过程如图 4 所示。由图 4 可知:当垮落岩体轴向应变 $\varepsilon=0$ 时,垮落岩体内的岩块以青色为主,其中直径为 0.8 m 的岩块组成的岩体的平均配位数为 5.1,随轴向应变的增大,垮落岩体内岩块间接触力增大,岩块间的连接网络越来越密实,使岩块的配位数也逐渐增大。当垮落岩体轴向应变为 $\varepsilon=0.25$ 时,垮落岩体内的岩块以红色为主,直径为 0.8 m 的岩块组成的岩体的平均配位数达 7.8。

将岩块配位数从小到大排列,统计垮落岩体内不同配位数岩块数目,求不同配位数岩块的分布频率,如图 5 所示。由图 5 可知:不同粒径岩块的配位数的频率分布整体均呈单峰结构。随配位数的增加,岩块的数量呈现先增加后降低的趋势。以直径为 0.8 m 的岩块组成的岩体为例,当垮落岩体轴向应变为 $\varepsilon=0$ 时,配位数为 5 的岩块占比最大。随

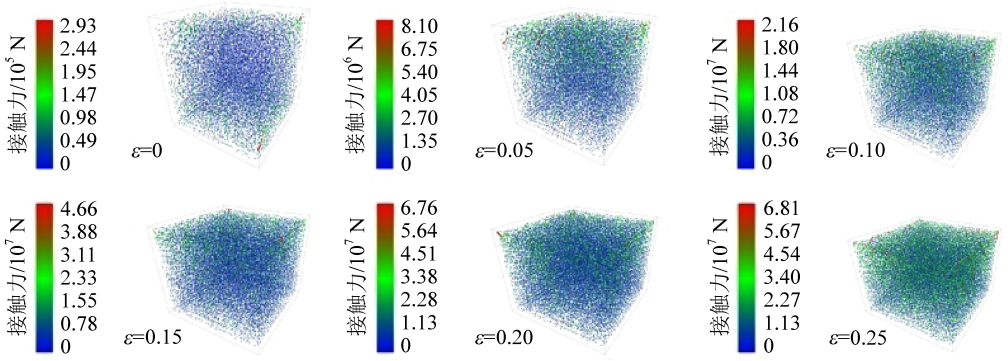

(a) D=0.6 m

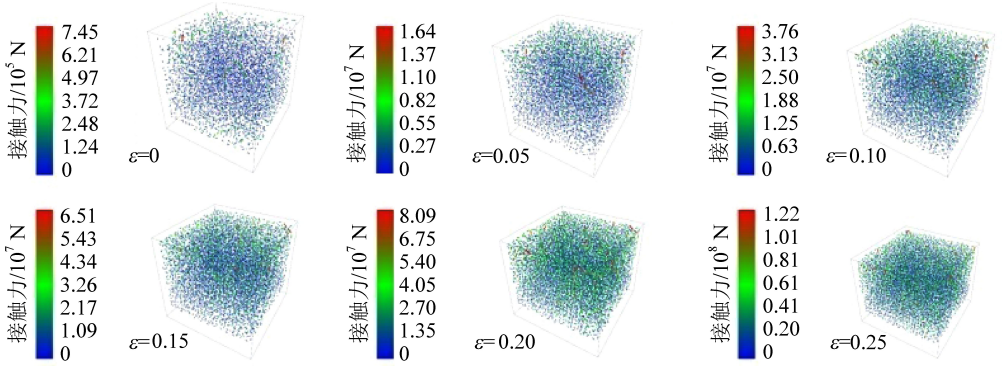

(b) D=0.8 m

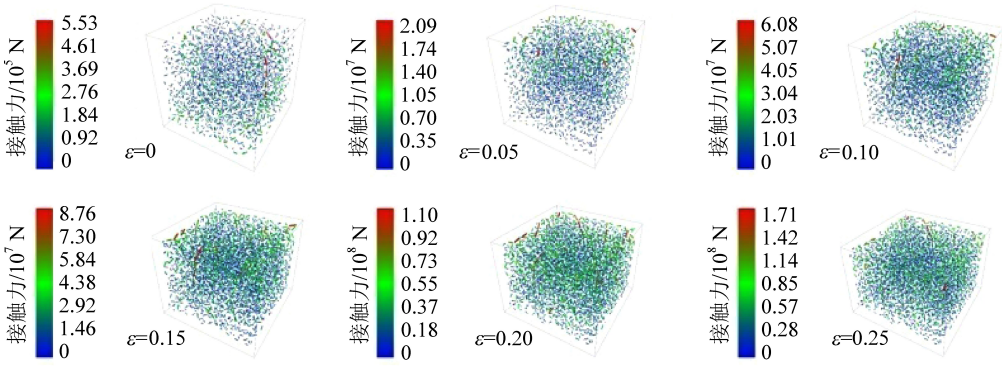

(c) D=1.0 m

图 2　岩块间接触力的演化

Fig.2　Evolution of contact forces between rock blocks

轴向应变的增大,岩块间的接触网络不断重组,使垮落岩体更密实,岩块配位数增加,单峰结构不断向右移动。当岩体轴向应变 $\varepsilon = 0.25$ 时,配位数为 9 的岩块占比最大。

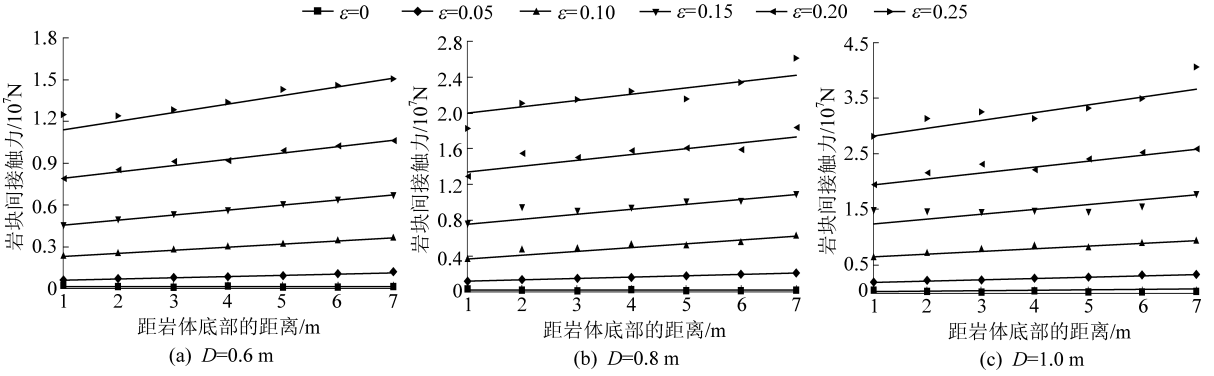

图 3　垮落岩体内不同层位岩块接触力的分布

Fig.3　Contact forces distribution of rock blocks in different layers of crushed rock mass

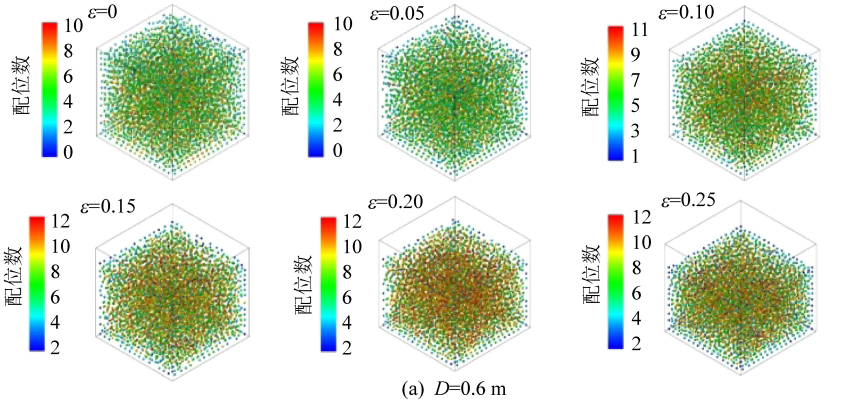

(a) D=0.6 m

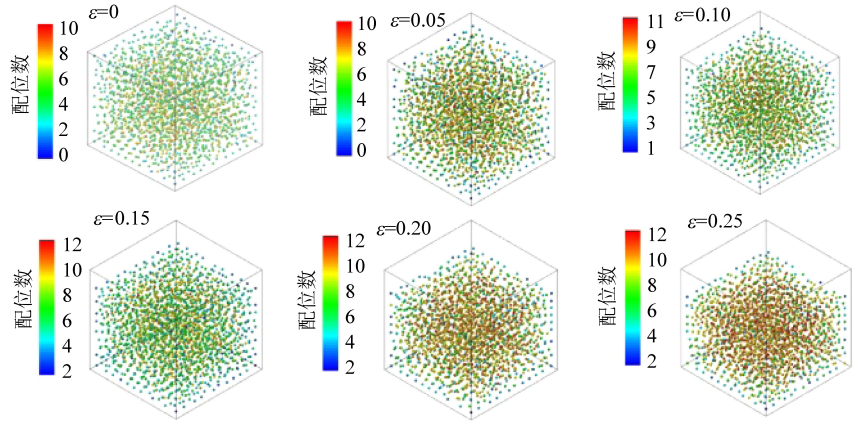

(b) D=0.8 m

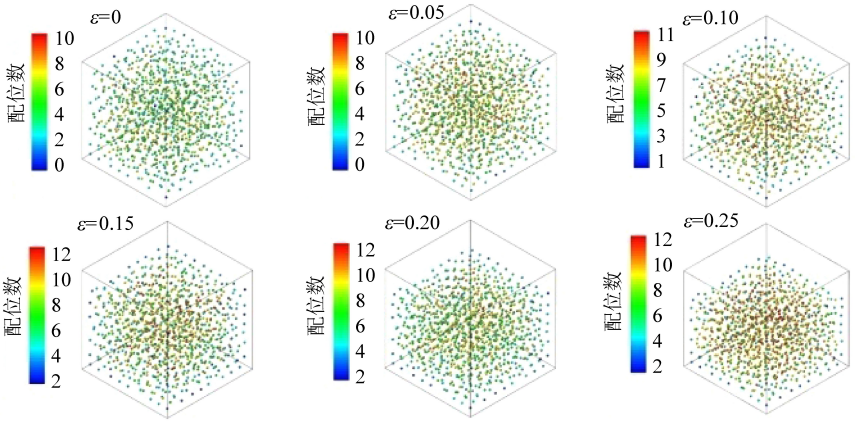

(c) D=1.0 m

图 4　配位数演化过程

Fig.4　Evolution of coordination number

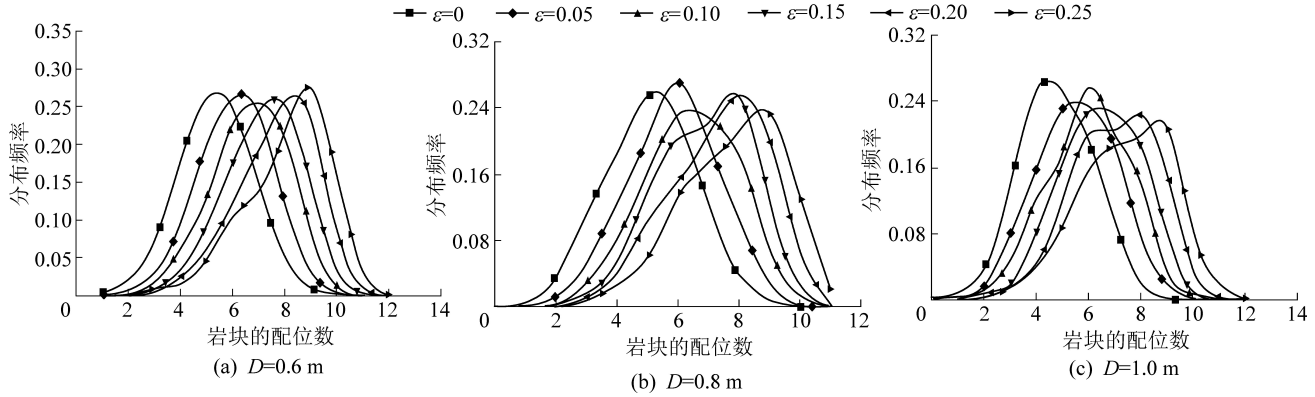

(a) D=0.6 m　(b) D=0.8 m　(c) D=1.0 m

图 5　岩块配位数的频率分布曲线

Fig.5　Probability density functions of coordination number of rock blocks

垮落岩体内不同层位岩块配位数的分布情况如图 6 所示。由图 6 可知:同一轴向应变下,岩块配位数自下而上先急剧增大,随后缓慢增加。因垮落岩体上部岩块的受力要大于下部,使垮落岩体下部岩块约束小,岩块堆积较松散,导致垮落岩体下部岩块配位数较小。相同层位垮落岩体,随轴向应变增加,垮落岩体越密实,导致垮落岩体内岩块配位数越大。

2.3　宏观尺度下垮落岩体的空隙率

不同层位垮落岩体空隙率的分布如图 7 所示。由图 7 可知:相同轴向应变下,垮落岩体空隙率自下向上先快速降低,随后缓慢降低,其中自垮落岩体底部向上 2 m 范围岩体的空隙率最大。以 $D=0.8$ m 的岩块组成的垮落岩体为例,当轴向应变为 0 时,垮落岩体底部空隙率是上部空隙率的 1.1 倍。由于垮落岩体下部岩块受到外部载荷扰动较小,岩块堆积较松散,导致轴向应变越大,垮落岩体上下层位空隙率的差值会越大,当岩体轴向应变为 0.25 时,岩体底部空隙率是上部空隙率的 1.4 倍。

垮落岩体空隙率、岩块平均配位数与轴向应变缩量之间的关系如图 8 所示。由图 8 可知:随轴向

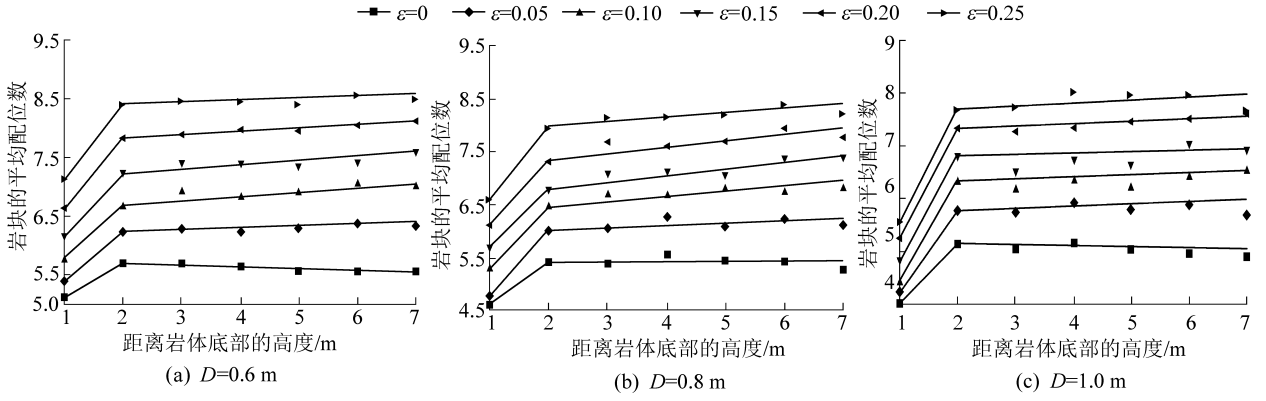

(a) D=0.6 m　(b) D=0.8 m　(c) D=1.0 m

图 6　垮落岩体内不同层位岩块的配位数的分布情况

Fig.6　Distribution of coordination numbers at different horizons of crushed rock mass

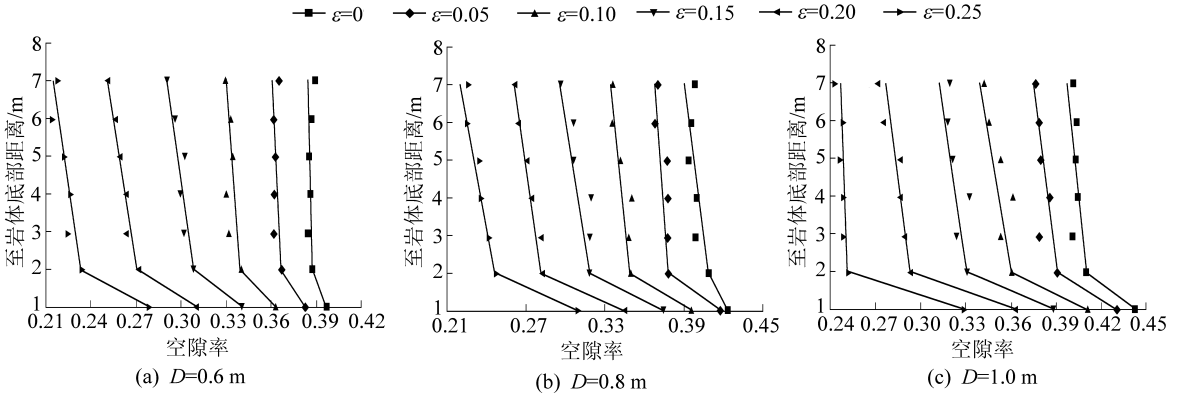

(a) D=0.6 m　(b) D=0.8 m　(c) D=1.0 m

图 7　不同层位岩体空隙率的分布

Fig.7　Distributions of voidage at different horizons

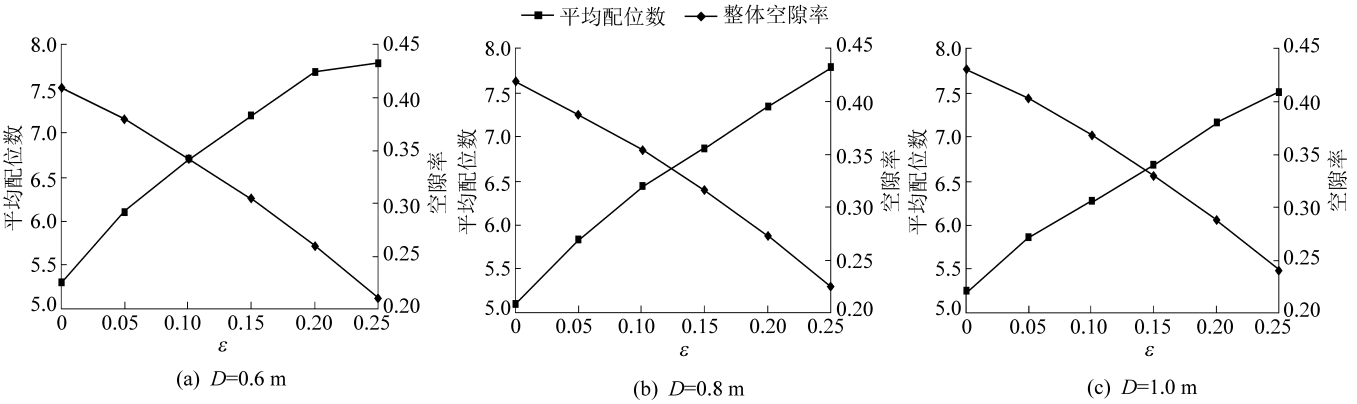

(a) D=0.6 m　(b) D=0.8 m　(c) D=1.0 m

图 8　配位数和空隙率随岩体轴向应变的变化

Fig.8　Curves of coordination number and voidage with aixal strain

应变的增大,垮落岩体内岩块的平均配位数逐渐增大,垮落岩体的空隙率逐渐降低。当垮落岩体轴向应变为 0%时,岩块的平均配位数较小,岩块堆积的较疏松,使岩块间的空隙较大。随轴向应变的增大,岩块的摩擦和挤压作用增强,岩块的配位数增大,岩块间的连接网络更加密实,使垮落岩体内的大空隙分裂成的小空隙,岩体内的空隙率降低。

3　效果验证

为了验证数值模拟结果的真实性,将本次数值模拟结果与已有的试验结果[28]进行了比较。已有的试验使用电液伺服控制测试系统 MTS815.02 对垮落岩块进行轴向压缩,测试不同轴向应变下岩体的空隙率如图 9 所示。由图 9 可知:数值模拟与试验 2 种方法得到的空隙率随轴向应变的变化规律高度吻合。随轴向应变的增大,岩体空隙率均呈现线性减小的趋势。进一步说明本次数值模拟的选择的方法、模型、及参数的合理性。

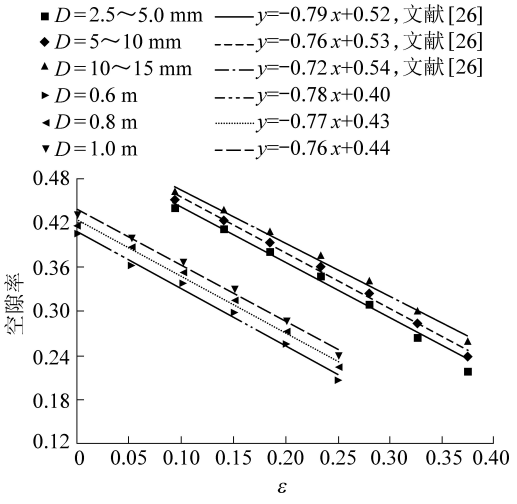

图 9　垮落岩体轴向应变与空隙率关系

Fig.9　Relationship between axial strain of crushed rock mass and voidage

4　结　　论

1)在外部载荷作用下,岩块间的挤压作用增强,导致岩块间的接触力增大。由于外部载荷无法从垮落岩体顶部的受力端均匀地传递到岩体下部,导致垮落岩体上部岩块受力要大于下部。随轴向应变增大,岩块间接触力较大的区域自垮落岩体上部向下不断扩展。

2)岩块配位数自下向上先急剧增大,随后缓慢增加。由于垮落岩体上部岩块的受力大于下部,使垮落岩体下部岩块堆积的较松散,配位数较小。随轴向应变增大,岩块受力越大,岩块间接触网络越密集,导致岩块的配位数不断增加。

3)垮落岩体自下向上空隙率先急剧降低,随后缓慢下降。由于垮落岩体下部岩块受到外部载荷扰动较小,岩块间的连接网络较松散,配位数最小,导致垮落岩体下部空隙率最大,其中下部空隙率是上部的 1.1～1.4 倍。

参考文献(References):

[1] ESTERHUIZEN Gabriel S,KARACANC Öezgen.A methodology for determining gob permeability distributions and its application to reservoir modeling of coal mine longwalls [J]. Sme Annual Meeting,2007,88(1):12-37.

[2] 汪北方,梁　冰,姜利国,等.采空区垮落岩体空隙储水分形计算及应用研究[J].岩石力学与工程学报,2015,34(7):1444-1451.
WANG Beifang, LIANG Bing, JIANG Liguo, *et al*. Research on fractal calculation and application of water storage in void of caving rock in goaf[J].Chinese Journal of Rock Mechanics and Engineering,2015,34(7):1444-1451.

[3] 孟召平,师修昌,刘珊珊,等.废弃煤矿采空区煤层气资源评价模型及应用[J].煤炭学报,2016,41(3):537-544.
MENG Zhaoping, SHI Xiuchang, LIU Shanshan, *et al*. Evaluation model of CBM resources in abandoned coal mine and its application[J].Journal of China Coal Society,2016,41(3):537-544.

[4] 郝元伟,杨　洋,涂　辉,等.煤矿封闭采空区瓦斯发电气源储量预测方法研究[J].煤炭科学技术,2019,47(6):151-157.
HAO Yuanwei,YANG Yang,TU Hui,*et al*.Research on prediction method of gas source reserve for gas power generation in closed goaf of coal mine [J]. Coal Science and Technology, 2019, 47(6): 151-157.

[5] YANG Wei,LIN Baiquan,YAN Qing,*et al*.Stress redistribution of longwall mining stope and gas control of multi-layer coal seams [J].International Journal of Rock Mechanics & Mining Sciences, 2014,72:8-15.

[6] PALCHIK Vyacheslav. Time-dependent methane emission from vertical prospecting boreholes drilled to abandoned mine workings at a shallow depth[J]. International Journal of Rock Mechanics and Mining Sciences,2014,72:1-7.

[7] 司俊鸿,程根银,朱建芳,等.采空区非均质多孔介质渗透特性三维建模及应用[J].煤炭科学技术,2019,47(5):220-224.
SI Junhong, CHENG Genyin, ZHU Jianfang, *et al*. Three-dimensional modeling and application of permeability characteristics of heterogeneous porous media in goaf [J].Coal Science and Technology,2019,47(5):220-224.

[8] 汪　东.回采工作面配风量对采空区漏风及自燃影响分析[J].煤炭科学技术,2016,44(12):96-101.
WANG Dong.Analysis on effect of air quantity of coal mining face to air leakage and spontaneous combustion in goaf [J]. Coal Science and Technology,2016,44(12):96-101.

[9] 赵洪宝,张　欢,王宏冰,等.采空区瓦斯体积分数区域分布三维实测装置研制与应用[J].煤炭学报,2018,43(12):3411-

3418.
ZHAO Hongbao, ZHANG Huan, WANG Hongbing, *et al*. Development and application of a three-dimensional measurement device for gas concentration[J]. Journal of China Coal Society, 2018, 43(12): 3411-3418.

[10] YANG Xiaochen, SASAKI Kyuro, ZHANG Xiaoming, *et al*. Permeability estimate of underground long-wall goaf from P-wave velocity and attenuation by lab-scale experiment on crushed rock samples[J]. Journal of Applied Geophysics, 2018, 159: 785-794.

[11] 陈占清,李顺才,茅献彪,等.饱和含水石灰岩散体蠕变过程中孔隙度变化规律的试验[J].煤炭学报,2006,31(1):26-30.
CHEN Zhanqing, LI Shuncai, MAO Xianbiao, *et al*. Experimental on porosity changing of water-saturated granular limestone during its creep[J]. Journal of China Coal Society, 2006, 31(1): 26-30.

[12] 樊秀娟,茅献彪.破碎砂岩承压变形时间相关性试验[J].采矿与安全工程学报,2007,24(4):486-489.
FAN Xiujuan, MAO Xianbiao. Experimental study of time-dependent deformation of broken sandstones under pressure[J]. Journal of Mining & Safety Engineering, 2007, 24(4): 486-489.

[13] 张季如,祝　杰,黄文竞.侧限压缩下石英砂砾的颗粒破碎特性及其分形描述[J].岩土工程学报,2008,30(6):783-789.
ZHANG Jiru, ZHU Jie, HUANG Wenjing. Crushing and fractal behaviors of quartz sand-gravel particles under confined compression[J]. Chinese Journal of Geotechnical Engineering, 2008, 30(6): 783-789.

[14] 孟召平,潘结南,刘亮亮,等.含水量对沉积岩力学性质及其冲击倾向性的影响[J].岩石力学与工程学报,2009,28(S1):2637-2643.
MENG Zhaoping, PAN Jienan, LIU Liangliang, *et al*. Influence of moisture contents on mechanical properties of sedimentary rock and its bursting potential[J]. Chinese Journal of Rock Mechanics and Engineering, 2009, 28(S1): 2637-2643.

[15] 梁运涛,张腾飞,王树刚,等.采空区孔隙率非均质模型及其流场分布模拟[J].煤炭学报,2009,34(9):1203-1207.
LIANG Yuntao, ZHANG Tengfei, WANG Shugang, *et al*. Heterogeneous model of porosity in gobs and its airflow field distribution[J]. Journal of China Coal Society, 2009, 34(9): 1203-1207.

[16] 徐俊明,张吉雄,黄艳利,等.充填综采矸石-粉煤灰压实变形特性试验研究及应用[J].采矿与安全工程学报,2011,28(1):158-162.
XU Junming, ZHANG Jixiong, HUANG Yanli, *et al*. Experimental research on compress deformation characteristic of waste-fly ash and its application in backfilling fully mechanized coal mining technology[J]. Journal of Mining & Safety Engineering, 2011, 28(1): 158-162.

[17] 苏承东,顾　明,唐　旭,等.煤层顶板破碎岩石压实特征的试验研究[J].岩石力学与工程学报,2012,31(1):18-26.
SU Chengdong, GU Ming, TANG Xu, *et al*. Experiment study of compaction characteristics of crushed stones from coal seam roof[J]. Chinese Journal of Rock Mechanics and Engineering, 2012, 31(1): 18-26.

[18] 王少锋,王德明,曹　凯,等.采空区及上覆岩层空隙率三维分布规律[J].中南大学学报(自然科学版),2014,45(3):833-839.
WANG Shaofeng, WANG Deming, CAO Kai, *et al*. Distribution law of 3D fracture field of goaf and overlying strata[J]. Journal of Central South University (Science and Technology), 2014, 45(3): 833-839.

[19] 冯梅梅,吴疆宇,陈占清,等.连续级配饱和破碎岩石压实特性试验研究[J].煤炭学报,2016,41(9):2195-2202.
FENG Meimei, WU Jiangyu, CHEN Zhanqing, *et al*. Experimental study on compaction of saturated broken rock of continuous gradation[J]. Journal of China Coal Society, 2016, 41(9): 2195-2202.

[20] WANG Shaofeng, LI Xibing, WANG Deming. Mining-induced void distribution and application in hydro-thermal investigation and control of an underground coal fire: a case study[J]. Process Safety & Environmental Protection, 2016, 102: 734-756.

[21] 孙利辉,纪洪广,蒋　华,等.弱胶结地层条件下垮落带岩层破碎冒落特征与压实变形规律试验研究[J].煤炭学报,2017,42(10):2565-2572.
SUN Lihui, JI Hongguang, JIANG Hua, *et al*. Experimental study on characteristics of broken caving and regularity of compaction deformation of rocks in caving zone in weakly cemented strata[J]. Journal of China Coal Society, 2017, 42(10): 2565-2572.

[22] 褚廷湘,李　晶,晁江坤,等.承压破碎煤体碎胀系数演变特征与机制[J].煤炭学报,2017,42(12):3182-3188.
CHU Tingxiang, LI Pin, ZHAO Jiangkun, *et al*. Bulking coefficient evolution characteristics and mechanism of compacted broken coal[J]. Journal of China Coal Society, 2017, 42(12): 3182-3188.

[23] 张俊文,王海龙,陈绍杰,等.大粒径破碎岩石承压变形特性[J].煤炭学报,2018,43(4):1000-1007.
ZHANG Junwen, WANG Hailong, CHEN Shaojie, *et al*. Bearing deformation characteristics of large-size broken rock[J]. Journal of China Coal Society, 2018, 43(4): 1000-1007.

[24] 杨永香,周　健,贾敏才,等.饱和砂土液化特性的可视化试验研究[J].岩土力学,2011,32(6):1643-1648.
YANG Yongxiang, ZHOU Jian, JIA Mincai, *et al*. Visualization testing on liquefaction properties of saturated sands[J]. Rock and Soil Mechanics, 2011, 32(6): 1643-1648.

[25] 孔　亮,陈凡秀,李　杰.基于数字图像相关法的砂土细观直剪试验及其颗粒流数值模拟[J].岩土力学,2013,34(10):2971-2978.
KONG Liang, CHEN Fanxiu, LI Jie. Meso-direct-shear test of sand based on digital image correlation method and its PFC numerical simulation[J]. Rock and Soil Mechanics, 2013, 34(10): 2971-2978.

[26] MA Dan, MIAO Xiexing, JIANG Guanghui, *et al*. An experimental investigation of permeability measurement of water flow in crushed rocks[J]. Transport in Porous Media 2014, 105(3): 571-595.